Monitoring Interfacial Bioelectrochemistry Using a FRET Switch

J. J. Davis,*,† H. Burgess,† G. Zauner,‡ S. Kuznetsova,‡ J. Salverda,§ T. Aartsma,§ and G. W. Canters‡

Central Research Laboratory, Mansfield Road, Department of Chemistry, University of Oxford, South Parks Road, Oxford OX1 3QR, United Kingdom, and Leiden Institute of Physics, Huygens Laboratory and Leiden Institute of Chemistry, Gorlaeus Laboratories, Leiden University, The Netherlands

Received: May 18, 2006; In Final Form: August 17, 2006

Generation of functionally active biomolecular monolayers is important in both analytical science and biophysical analyses. Our ability to monitor the redox-active state of immobilized proteins or enzymes at a molecular level, from which stochastic and surface-induced variations would be apparent, is impeded by comparatively slow electron-transfer kinetics and associated signal:noise difficulties. We demonstrate herein that by covalently tethering an appropriate dye to the copper protein azurin a highly oxidation-state-sensitive FRET process can be established which enables redox switching to be optically monitored at protein levels down to the zeptomolar limit. The surface-potential-induced cycling of emission enables the redox potential of clusters of a few hundred molecules to be determined.

Introduction

Protein electrochemical studies have led not only to an enhanced understanding of the important role these molecules play in biological energy transduction processes (including structure/function correlations) but also, in cases where an understanding has suitably matured, to significant biosensing developments.[1] Reliable heterogeneous electron transfer of metalloproteins at manmade electrode surfaces is achievable only through careful consideration of protein and electrode surface chemistry, and much progress has been made since the pioneering work of Hill and Yeh.[2,3] Specifically, many studies have centered on modifying the electrode surface such that its physicochemical interactions with the protein "model", to variant levels of simplification, the natural interfacial interactions of the protein in its native environment. It can be particularly advantageous, in these studies, to confine voltammetric investigations to the electrode surface, thereby removing complicating diffusion-based contributions to voltammetry.[4,5] These interfacial analyses have advanced to the point where detailed kinetic and thermodynamic investigations including quantitative electronic coupling (such as structure and distance dependency) experiments and reorganization can be robustly pursued.[5] Voltammetric investigations, though powerful, are not adequate to define the inherently variable and complex interfacial processes responsible for signal generation. The faradaic responses are additionally (and largely without exception) averaging over typically $10^{10}-10^{14}$ of such interfacial redox interactions (depending on surface coverage and electrode area). In many bioelectrochemical investigations voltammetric data deviates from ideality by quite a considerable margin; specifically, peak separations and widths are commonly observed to be large. These characteristics may be ascribable to the heterogeneities inherent at the surface but are not resolvable in bulk analyses. Though surface reactions at electrodes can be probed by methods such as surface-enhanced resonance Raman spectroscopy (SERRS), ellipsometry, and IR spectroscopy, none of these techniques is able to provide direct real-space or molecularly resolved information. Ideally, it is exactly this level of detail that is required when modeling or interpreting a voltammetric response. Experiments capable of systematically examining data available from single or low multiples of molecules are attractive because they reveal heterogeneities not evident in bulk assays. Though the spatial resolution of fluorescence methods is comparatively low, the high signal:noise data acquirement accessible with appropriate dyes facilitates optical resolutions at the single-molecule scale. Development of wide-field total internal reflection fluorescence (TIRF) microscopes coupled with high-sensitivity CCD cameras, in particular, has enabled the data to be gathered on individual surface-confined molecular species.[6,7] In coupling emission and redox characteristics within such an experimental configuration it should be possible to resolve electrochemical events at molecular levels.

Fluorescence resonance energy transfer (FRET) is the radiationless transfer of energy from an excited donor to a suitable acceptor fluorophore, a physical process which depends on effective spectral overlap and appropriate fluorophore dipole alignment. The phenomenon, which is characterized by a decrease in donor emission and simultaneous (sensitized) increased acceptor emission, is highly distance dependent and, as such, can be used to measure both protein−protein interactions and conformational fluctuations within suitably labeled individual molecules. The latter has been resolved down to the level of the single molecule.[8] In this study a donor dye moiety is attached to the external surface of the protein through a solution-exposed (engineered) cysteine or N-terminal residue. The FRET phenomenon in this case is not used to monitor changes in distance or conformation but a change in redox state. The copper redox cofactor functions as the energy acceptor, facilitating the establishment of a redox-state-dependent FRET switch (Scheme 1).

Azurin is a well-characterized, 14 kDa, blue copper protein involved in bacterial electron-transfer chains, such as those in *Pseudomonas aeruginosa,* where it is now believed to play a

† University of Oxford.
‡ Leiden Institute of Chemistry, Leiden University.
§ Leiden Institute of Physics, Leiden University.

10.1021/jp0630525 CCC: $33.50
Published on Web 09/28/2006

SCHEME 1: Diagrammatic Representation of the FRET-Based, Redox-State-Sensitive Fluorescence Switch[a]

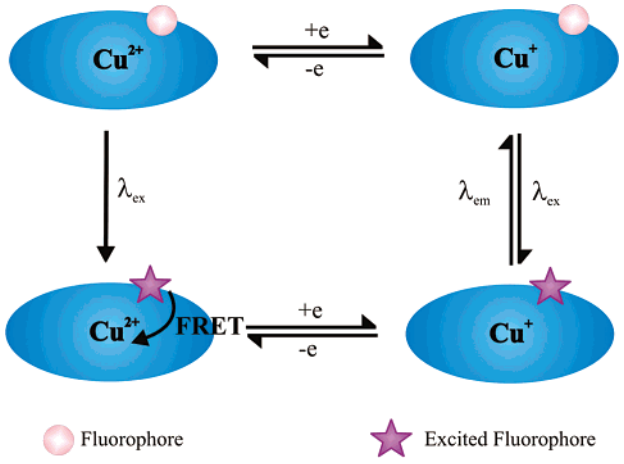

[a] The covalently attached fluorophore is excited at a wavelength close to it's extinction maximum, λ_{ex}. In the reduced form of the protein the fluorophore relaxes by the conventional route, with emission of a photon at a characteristic wavelength, λ_{em}. In the oxidized form of the protein a FRET process can occur between the excited fluorophore and the copper redox center, resulting in loss of fluorescence emission.

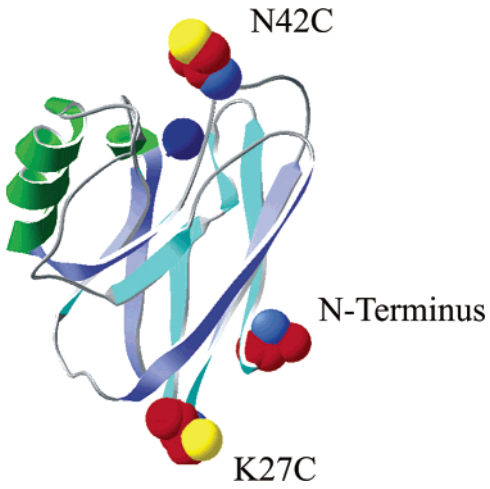

Figure 1. Schematic representation of Azurin adapted from PDB 5AZU using swiss-pdb viewer (GSK). The copper cofactor is shown as a blue sphere; positions of engineered cysteines (27C, 42C) available for labeling are shown.

role in the oxidative stress response (Figure 1).[9] Though the wild-type form of azurin can be immobilized on pristine gold electrode surfaces through its exposed disulfide moiety, previous studies have reported that such arrays are electrochemically inactive.[10] Cysteine mutants can be robustly and physically adsorbed onto alkyl-terminating thiol adlayers in a way which facilitates both facile electron transfer and site-specific fluorophore labeling. In its oxidized form the protein displays a strong ($\epsilon = 5.6$ mM^{-1} cm^{-1}) absorption in the 550−650 nm range (Figure 2), which corresponds to a charge-transfer transition involving mainly the $d_{x^2-y^2}$orbital on the Cu and a 3p orbital on the Cys112 sulfur. This absorption disappears when the Cu site is reduced and attains a d^{10} electronic configuration.

In previous work, the basic principle of using FRET to monitor protein redox-state change has been demonstrated.[11,12] We extend this work herein by driving this switching reversibly at optically transparent electrode surfaces on which arrays of dye-labeled proteins have been immobilized. An in situ electrochemical-TIRF configuration has been used to correlate emission from surface-confined molecules with voltammetric

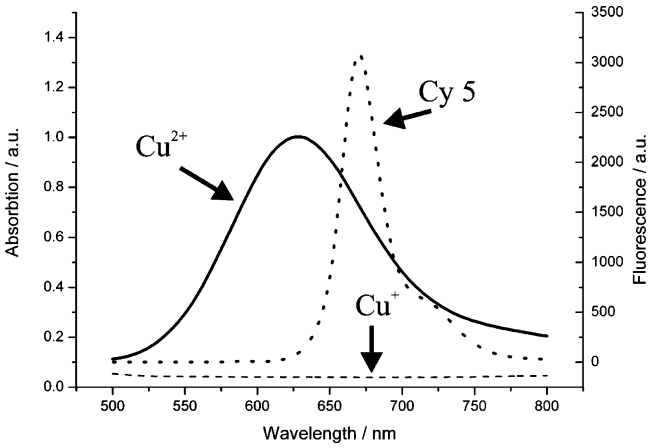

Figure 2. Overlap for the azurin Cu^{2+} Cy5 FRET pair. The Cy5 emission spectrum (dotted line) was determined at an excitation wavelength λ_{ex} 600 nm. UV−vis absorption spectra of oxidized (Cu^{2+}) wt azurin (solid line) and reduced (Cu^{+}) wt azurin (dashed line). Reducing agent DTT. All spectra were determined in 100 mM phosphate buffer pH 7.0.

signals. In this way, bioelectrochemical switching, optically tracked, has been performed at the 10^{-21} molar level.

Experimental Section

Preparation and purification of wild-type Cu and Zn proteins and the mutants N42C and K27C was carried out according to published procedures.[13] Prior to labeling, protein solutions were incubated with TCEP (Tris[2-carboxyethyl] phosphine hydrochloride covalently linked to a 4% cross-linked beaded agarose support) gel (Pierce, U.K.), according to the manufacturer's instructions, to reduce any dimers present.

Labeling at the N Terminus (all proteins). A 10 μL aliquot of Cy5-NHS ester (~1 M) (Amersham Biosciences, U.K.) in DMSO was added to a freshly reduced solution of azurin (dye: azurin ratio approximately 2:1; 100−300 μM) in 20 mM HEPES buffer, pH 9.0. After a 2 h incubation at room temperature, excess dye was removed by centrifugal filtration (Microcon YM-3, Millipore, U.K.; 3 kDa cutoff). Labeled protein was diluted with 20 mM KH_2PO_4/K_2HPO_4 buffer, pH 7.0, with final concentrations determined by UV−vis spectroscopy.

Labeling at the Thiol Residue (N42C and K27C). A 10 μL aliquot of Cy5-maleimide (Amersham Biosciences, U.K.) in DMSO was added to a freshly reduced solution of azurin (100−300 μM) in 20 mM KH_2PO_4/K_2HPO_4, buffer pH 7.0. After a 2 h incubation at room temperature and overnight incubation at 4 °C, excess dye was removed by centrifugal filtration.

Solution (Bulk) Chemical Switching. The fluorescence of 1 μM solutions of labeled proteins was recorded using a Hitachi F-4500 fluorescence spectrophotometer. The excitation wavelength was 603 nm; emission was recorded between 500 and 700 nm. The oxidation state of the protein was altered by addition of aliquots of freshly prepared DTT (100 mM) and $K_3Fe(CN)_6$ (10 mM) in Millipore water (18.2 MΩ cm).

Electrode Preparation. Planar electrodes (5 mm × 15 mm) were cut from optically transparent gold (10 nm evaporated onto glass cover slides with a chromium adhesion layer; manufactured in house). The surfaces were cleaned by sonicating in Decon solution and ethanol for 15 min each. The clean gold was annealed at 200 °C for at least 24 h. Electrodes were formed by attaching copper wire to one end of the gold electrode with silver conductive paint (RS,U.K.); the joint was insulated with epoxy resin. Further cleaning was carried out by electropolishing

in 1 M H_2SO_4 between −0.2 and 1.6 V vs a standard calomel electrode (SCE). The electrodes were immediately immersed in a 5 mM ethanolic solution of heptanethiol (Fluka, Gillingham, U.K.) for a minimum of 15 h. Excess thiol was removed by rinsing with ethanol and water. Protein self-assembly was carried out by incubating the freshly rinsed, thiolated electrode with a solution of azurin (1−10 μM) at 2−4 °C for at least 2 h. Unbound protein was removed by rinsing with water immediately prior to use. Electrodes for combined TIRF and electrochemistry were prepared in an analogous manner. The dimensions of the gold in this case are 14 × 14 mm; after the annealing step the gold was glued over the hole of a Petri dish (MatTek, Ashland, MA). The joints were insulated with electrical tape.

Electrochemistry. Cyclic voltammetry was carried out with a μ-Autolab potentiostat (Windsor Scientific, Slough, U.K.) at a range of scan rates (1−9000 mV/s) between −0.5 and +0.5 V vs SCE. The counter electrode was Pt gauze, and the supporting electrolyte solution was 100 mM KH_2PO_4/K_2HPO_4, pH 7.0.

Total Internal Reflection Fluorescence Microscopy. Samples were mounted on a Nikon TE2000-E microscope with a TIRF module (Nikon, U.K.). The sample was excited with 594 nm HeNe laser (JDS Uniphase, San Jose, CA), through an ×100 magnification, oil immersion, TIRF objective. Emitted light was filtered through a dichroic mirror (660 nm, LP) and an (700/75 nm) band-pass filter and recorded with a back-illuminated iCCD camera (Andor, Belfast, Northern Ireland).

TIRF under Potential Control. A single-compartment electrochemical cell, consisting of a functionalized transparent gold working electrode, SCE reference electrode, and Pt gauze counter electrode was assembled above the Nikon TE2000-E microscope and filled with degassed KH_2PO_4/K_2HPO_4 electrolyte, pH 7.0. Fluorescence images were recorded as time-resolved sequences, across 300 × 100 ms exposures, at a frame rate of 3 Hz. During this period the working electrode surface voltage was swept between −0.5 and 0.5 V vs SCE at a rate of 400 mV/s. Typically, 10 full cycles of potential were completed (photobleaching across this time frame results in an emission decrease from sampled pixels of some 20%).

Protein-dye distances, *R*, were determined from the protein crystallographic structure (PDB 5AZU)[14] using the measure function of the swiss-pdb viewer software.

Results and Discussion

(a) Protein Labeling and Characterization. Wild-type Cu and Zn forms of azurin and the mutants N42C and K27C were labeled, via the N-terminal amine or introduced surface cysteine group, with thiol-reactive maleimide or amine reactive NHS ester derivatives of Cy5 (660 nm emission) where appropriate. Cy5 was selected as an appropriate FRET donor due to the good spectral overlap between its emission and the oxidized protein absorption (Figure 2).The dye:protein labeling ratio was 1:0.7−1.2, as estimated from the protein absorption at 280 nm (ϵ = 19.6 or 9.8 mM^{-1} cm^{-1})[15] and the dye absorption at 650 nm (ϵ = 250 mM^{-1} cm^{-1}). Fluorescence emission was observed to be stable over continued exposure to 649 nm light with less than 0.4% signal decrease due to photobleaching over 60 s. The fluorescent conjugates remained stable in buffered solution over several months.

(b) Solution-Phase Redox-Linked FRET. Titration of the labeled proteins with aliquots of ferricyanide oxidant led to a significant decrease in fluorescence emission. Subsequent titration with the reducing agent dithiothreitol restored the

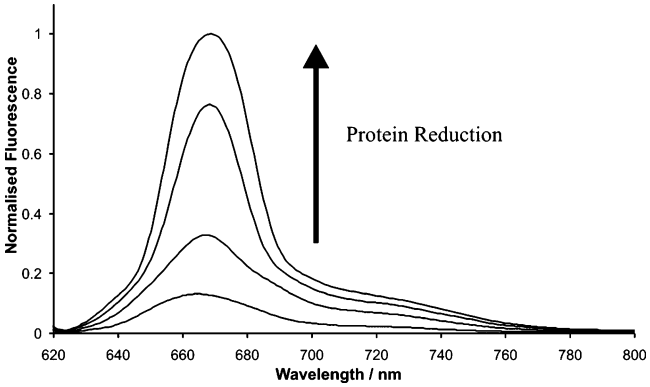

Figure 3. Chemical reduction of N42C Cu−NH_2 Cy5. A 1 μM solution in 100 mM phosphate buffer pH 7 was titrated with aliquots of 1 mM DTT. λ_{ex} = 600 nm. Data are normalized to the maximum fluorescence emission.

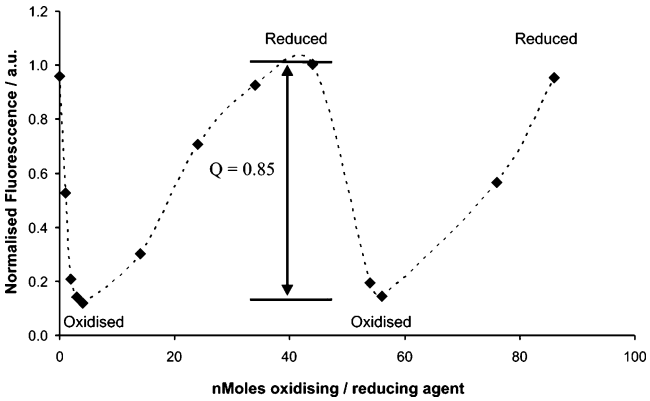

Figure 4. Reversibility of the FRET-based switch. Chemical oxidation and subsequent reduction of a 1 μM solution of N42C Cu Cye labeled at the N terminus in 100 mM phosphate buffer, pH 7.0. Titrated with aliquots of DTT and $K_3Fe(CN)_6$ (10 and 100 mM). Fluorescence emission and excitation = 660 and 600 nm, respectively.

fluorescence (see Figures 3 and 4). The extent of quenching observed was quantified by the FRET-based quenching ratio, *Q*, where

$$Q = 1 - F_{Ox}/F_{Red} \quad (1)$$

with F_{Ox} and F_{Red} being the fluorescence emission associated with the oxidized and reduced forms of the protein, respectively. *Q* varies predictably as a function of distance, *R*, between the fluorescent label and the copper redox center, with the fluorescence of N42C Cu mutant labeled at the cysteine residue, having a greater dependence upon oxidation state than the label on the more remotely located K27C Cu. The quenching ratio was not observed to vary significantly for mutants labeled at the N terminus. Control experiments carried out with either the nonredox active zinc form of labeled wt Cu or the Cy5 dye alone showed no dependency of emission on the presence of either of the solution-phase redox agents. The Förster radius (at which the energy transfer is 50% efficient) for this FRET pair can be determined as 2.8−3.2 nm (Table 1) from

$$Q = R_0^6/(R_0^6 + R^6) \quad (2)$$

from the solution FRET-based quenching value, *Q*, and the distance between the donor dye position and copper acceptor, *R* (see eqs 1 and 2).[16] The FRET quenching ratio associated with the N-terminus-labeled protein is higher than would be theoretically predicted from the crystallographic separation of

TABLE 1: Solution-Phase FRET Characteristics of the Azurin Forms Used in This Study[a]

azurin	label	R (nm)	Q	R_o (nm)
N42C Cu	N terminus	2.4	0.82 ± 0.15	3.13
Wt Cu	N terminus	2.4	0.77 ± 0.3	2.94
Wt Zn	N terminus	2.4	0.00 ± 0.04	N/A
N42C Cu	42 cysteine	1.0	0.77	1.49
K27C Zn	N terminus	2.4	0.49 ± 0.15	2.78
Cy5 Dye	NA	NA	0.00 ± 0.04	N/A

[a] Q is the FRET based quenching ratio, R the distance between the copper center and the amino acid carrying the fluorescent label, and R_0 the calculated Forster distance for these proteins. Errors in Q and calculated R_o are ± 3 standard deviations of the mean.

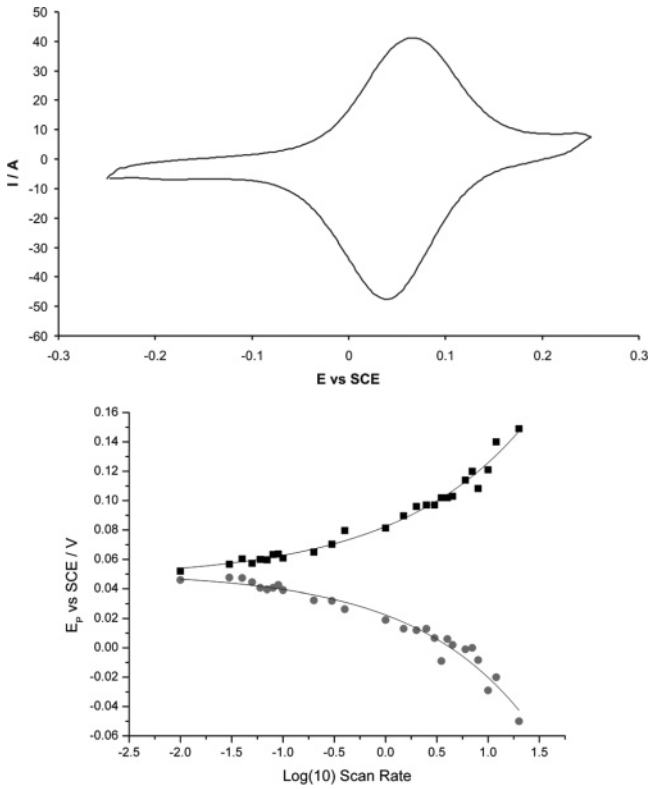

Figure 5. (top) Voltammetric response (100 mV/s) of N42C Cu azurin Cy5 labeled at the N terminus and immobilized on a transparent Au working electrode via a heptanethiol SAM. Reference electrode SCE, counter electrode Pt, electrolyte 100 mM phosphate buffer pH 7.0. (bottom) Change in anodic (diamonds) and cathodic (circles) peak positions with scan rate (sweep rates 25−8000 mV/s).

the residue and copper center, implying, possibly, considerable conformational flexibility in this protein region or flexibility in the linker by which the dye is attached to the protein framework.

(c) Surface-Confined Voltammetry. In recent years we and others have developed methods whereby metalloproteins can be assembled on electrode surfaces in well-defined, electrochemically addressable, molecular arrays.[10,17−19] Azurin possesses a hydrophobic region close to the copper site which can be utilized in attaining robust physisorption to alkyl-terminated thiolate SAMs.[20] On incubating heptanethiol-modified transparent Au electrodes in low micromolar concentration solutions of dye-labeled azurin for 15 h at 4 °C, protein adlayers could be generated from which robust and highly reproducible electrochemical responses could be obtained (Figure 5). Electroactive surface coverages were estimated, from integration of the Faradaic response, to be $\sim 5 \times 10^{10}$ molecules cm^{-2}, a value broadly in line with ranges previously reported for this interfacial system.[20,21] The midpoint redox potential of the N42C−Cy5 adlayer was 60−80 mV vs SCE, a value close to that obtained diffusively of wild-type unlabeled protein at EPG,[22] indicating minimal perturbation of structure at the interface. Voltammetric peak separations and widths (fwhm) were, respectively, 20 and 70−100 mV at slow scan rates, observations consistent with previous analyses.[23,24] Electron-transfer kinetics, determined through application of Laviron's theory to observations of peak divergence with voltage sweep rate (Figure 5), were observed to be 50−100 s^{-1}, in good agreement with previously reported determinations at equivalent interfacial configurations (Table 2).[20]

TABLE 2: Electrochemical Characteristics of the Protein Layers Studied[a]

azurin	$E_{1/2}$ (mV) vs SHE	surface coverage (10^{10}) (molecules cm^{-2})	I_{pa}/I_{pc}	ΔE_p (mV)	k_{et} (s^{-1})
N42C Cu	310−345	1−25	1.0−1.2	10−60	10−60
Wt	300−305	2−18	1.0−1.2	10−46	50−140

[a] Electron-transfer rate constants were determined from the variation in peak potential separation with scan rate from Laviron theory.[31] These adlayers were formed from 1.0−3.0 μM solutions.

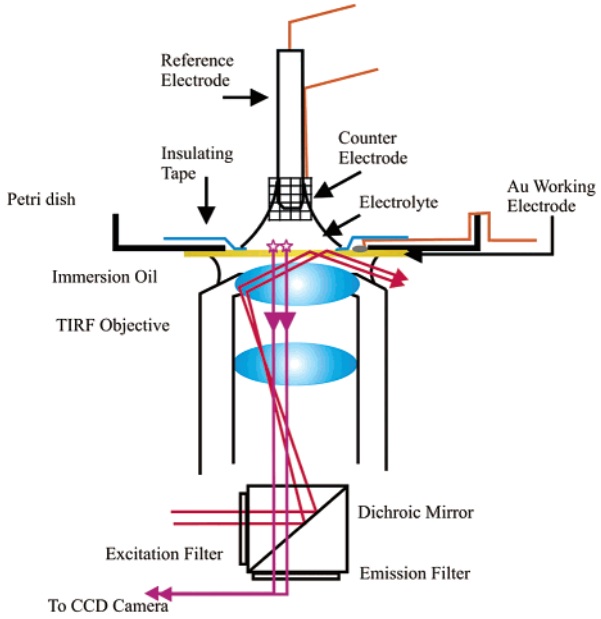

Figure 6. Schematic representation of the "electrochemical-TIRF" experimental configuration. A homemade, single-compartment electrochemical cell is fixed above the TIRF objective of a Nikon Te2000-E fluorescence microscope.

(d) Redox-Linked Surface-Confined FRET. Adlayers of Cy5-labeled N42C and wild-type Cu and Zn azurin were prepared on heptanethiol SAMs as previously discussed[25] and subject to initial electrochemical and AFM before being incorporated into an electrochemical TIRF configuration (Figure 6). On application of an appropriate triangular wave surface potential to a working transparent Au electrode fluorescence emission from the surface-confined protein is observed to be modulated, being 40−60% higher at potentials cathodic of the half-wave potential (Figures7 and 8). Control experiments with the dye alone and Cy5-labeled non-redox-active Zn N42C or wild-type protein layers showed less than 4% variance in emission across a broad range of surface potentials (Figure 8). A 5−15% degradation in emission intensity from sampled molecular clusters occurs over the time scale of 10 voltage

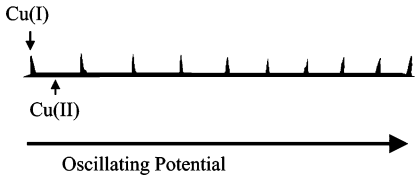

Figure 7. 3D representation of 10 complete cycles of surface potential. Each cluster constitutes approximately 1000 azurin N42C Cu molecules labeled at the N terminus with Cy5 NHS ester immobilized on a heptanethiol monolayer on optically transparent gold working electrode. Reference electrode SCE, counter electrode Pt, electrolyte 100 mM potassium phosphate buffer pH7. Sweep rate 0.4 mV/s. Exposure time = 100 ms. Scan range = 0.5−0.5 V vs SCE.

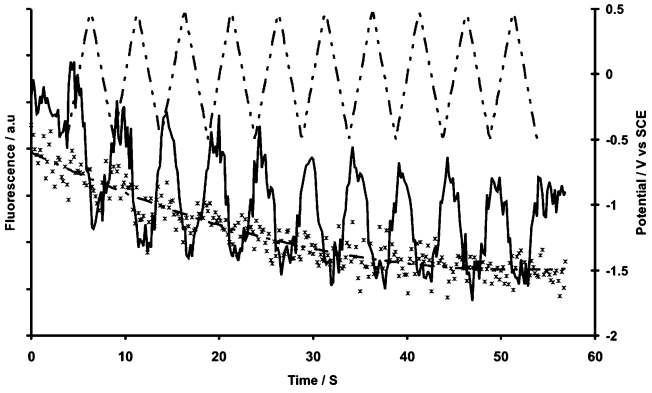

Figure 8. Potential-modulated fluorescence of N42C Cu−NH_2 Cy5 (solid line) immobilized on transparent Au via a heptanethiol monolayer. The potential was cycled between 0.5 and −0.5 V vs SCE at a scan rate of 0.4 V/s. Counter electrode Pt gauze, electrolyte 100 mM phosphate buffer pH 7.0. A control using the zinc inactive form of the wild-type protein (crosses) deviates by less than 4%, i.e., within the noise, over the same potential range.

sweeps at 0.4 V/s, implying that some 50−100 potential cycles are accessible prior to full photobleaching and consequent signal loss.

The FRET-based quenching ratio, *Q*, for surface-confined Cy5-N42C is low (∼0.46 ± 0.18) in comparison to that observed in solution (∼0.83 ± 0.13). This is likely to be reflective of both the different requirements associated with fluorescence emission and redox assays and effects associated with confining the protein to a surface. At the electrode surface appreciable quenching is expected to be associated with configurations in which electronic/redox coupling is likely to be most facile.[26] Though currently the subject of ongoing work, this may lead to a reduced *Q* (the emission signal being weighed somewhat in favor of proteins which are not being addressed electrochemically). It is, additionally, likely that the mobility of the label and, thereby, its average distance to the redox center, may differ when the protein is immobilized than when it is in solution. Finally, it should also be noted that the *Q* value observed for fluid-phase proteins labeled at the N terminus is somewhat higher than that expected based on crystallographically determined distances between the copper acceptor and the fluorophore donor (by some 25% based on an extrapolation of data obtained in solution with N42C- and K27C-labeled mutants).

The voltammetric response shown in Figure 5, with its associated half-wave potential and electron-transfer rate constant characteristics, is that summed across the entire electrochemically active surface and constitutes an average over all addressed molecules (some 10^{10} molecules). From each emission data set, each sampling some 1000 molecules on average, we can define a "half-wave potential" based on emission intensity as $E_{1/2}^{f}$,

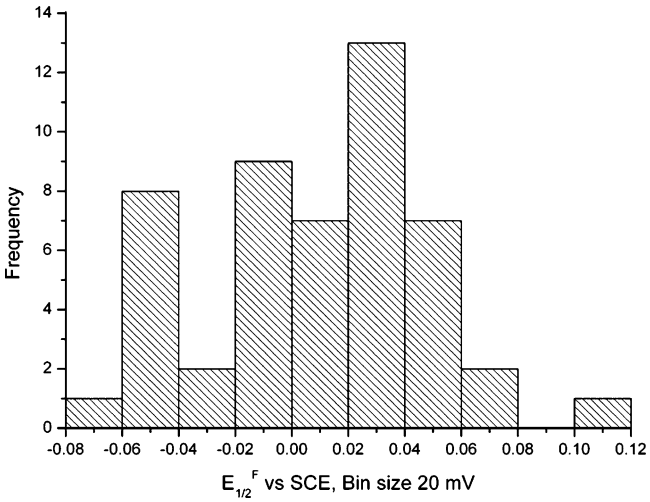

Figure 9. Histogram of $E_{1/2}^{f}$ values, determined from 50 sets of fluorescence emission data for N42C Cu molecules labeled at the N terminus as the potential is swept between −0.5 and 0.5 V vs SCE (scan rate = 0.4 V/s).

where $E_{1/2}^{f} = (E_{off} + E_{on})/2$ and E_{off} and E_{on} are the surface potentials corresponding to emission intensity being 50% of the maximum observed in the anodic or cathodic sweeps, respectively. In analyzing emission from 60 data sets (each sampling some 1000 molecules), $E_{1/2}^{f}$ is resolved as +6 ± 0.6 mV vs SCE (a value in good agreement with the voltammetrically derived half wave). The observation that $E_{1/2}^{f}$, as determined in this way, spans some 150 mV is potentially significant (Figure 9); the inherent heterogeneities associated with confining proteins to macroscale electrode surfaces have long been considered to be potentially important but cannot be resolved by standard electrochemical methods (the electrochemical half-wave potential is, of course, the average of that associated with all sampled molecules, typically some $10^{11}-10^{12}$ proteins).

Summary

Recently Holmes and Adams demonstrated the use of a confocal configuration to examine the photoinduced electron transfer associated with perylene chromophores and ITO electrodes. Though developmentally significant, this (nonbiological) redox change was shown to be neither reversible nor electrochemically (externally) driven.[27] Very recently, Yan et al. demonstrated the redox-linked fluorescence emission of NADH analogues.[28] Though single-molecule electrochemical detection has been achieved impressively within the confines of a scanning electrochemical microscope (SECM), such experiments do not involve direct current measurement nor are they readily extendable to bioelectrochemical systems.[29,30]

In this work we have been able to immobilize blue copper proteins appropriately tagged for FRET observations, drive their redox switching electrochemically, and simultaneously monitor concurrent modulation of fluorescence emission. Robust and highly reproducible surface-potential-induced optical switching has been observed on immobilizing appropriately tagged redox-active copper azurin molecules on short-chain alkanethiols SAMs on optically transparent thin film gold electrodes. Though the quenching characteristics of evaporated gold film ultimately hinder analyses at the single-molecule level, a comparison of the observed fluorescence emission from clusters of labeled proteins, with the emission from single labeled proteins immobilized on a nonquenching glass substrate, leads to the conclusion (after a calibrated weighting for the lower transmis-

sion of the Au substrate) that only ~1000 molecules are being optically sampled (2×10^{-21} mol); this represents an increase in "electrochemical resolution" of some $10^{7-}10^{8}$ orders of magnitude. In optically sampling different regions of the macroscale electrode surface, the half-wave potential for this protein is observed to span some 150 mV. This observation, undoubtedly related to protein fold or physiochemical heterogeneities across the surface, may be of considerable importance in our interpretation of macroscale bioelectrochemical signals.

References and Notes

(1) Cass, A.; Davis, G.; Francis, G.; Hill, H.; Aston, W.; Higgins, I.; Plotkin, E.; Scott, L.; Turner, A. *Anal. Chem.* **1984**, *56*, 667.

(2) Eddowes, M. J.; Hill, H. A. O. *J. Chem. Soc., Chem. Commun.* **1977**, 771.

(3) Yeh, P.; Kuwan, T. *Chem. Lett.* **1977**, 1145.

(4) Armstrong, F. A. Probing metalloproteins by voltammetry. In *Structure and Bonding*; Springer-Verlag: Berlin, 1990; Vol. 72, p 137.

(5) Armstrong, F. A.; Heering, H. A.; Hirst, J. *Chem. Soc. Rev.* **1997**, *26*, 169.

(6) Moerner, W. C.; Fromm, D. P. *Rev. Sci. Instrum.* **2003**, *74*, 3597.

(7) Funatsu, T.; Harada, Y.; Tokunaga, M.; Saito, K.; Yanagida, T. *Nature* **1995**, *374*, 555.

(8) Ha, T. *Single Mol.* **2001**, *2*, 283.

(9) Vijgenboom, E.; Busch, J. E.; Canters, G. W. *Microbiology* **1997**, *143*, 2853.

(10) Davis, J. J.; Bruce, D.; Canters, G. W.; Crozier, J.; Hill, H. A. O. *J. Chem. Soc., Chem. Commun.* **2003**, 576.

(11) Schmauder, R.; Alagaratnam, S.; Chan, C.; Schmidt, T.; Canters, G. W.; Aartsma, T. J. *J. Biol. Inorg. Chem.* **2005**, *10*, 683.

(12) Kuznetsova, S.; Zauner, G.; Schmauder, R.; Mayboroda, O. A.; Deelder, A. M.; Aartsma, T. J.; Canters, G. W. *Anal. Biochem.* **2006**, *350*, 52.

(13) Kamp, M. v. d.; Hali, F. C.; Rosato, N.; Agro, A. F.; Canters, G. W. *Biochim. Biophys. Acta* **1999**, *1019*, 283.

(14) Nar, H.; Messerschmidt, A.; Huber, R.; Kamp, M. v. d.; Canters, G. W. *J. Mol. Biol.* **1991**, *221*, 765.

(15) Kolczak, U.; Dennison, C.; Messerschmidt, A.; I, G. W. C. In Handbook of Metalloproteins; Messerschmidt, A., Huber, R., Poulos, T., Wieghardt, K., Eds.; John Wiley & Sons: Chichester, 2001.

(16) Lakowicz, J. R. *Principles of Fluorescence Spectroscopy*, 2nd ed.; 1999; Chapter 13.

(17) Song, S.; Clark, R. A.; Bowden, E. F. *J. Phys. Chem.* **1993**, *97*, 6564.

(18) Davis, J. J.; Morgan, D. A.; Wrathmell, C. L.; Axford, D. N.; Zhao, J.; Wang, N. *J. Mater. Chem.* **2005**, *15*, 2160.

(19) Zhang, J.; Chi, Q.; Kuznetsov, A. M.; Hansen, A. G.; Wackerbarth, H.; Christensen, H. E. M.; Andersen, J. E. T.; Ulstrup, J. *J. Phys. Chem. B* **2002**, *106*, 1131.

(20) Chi, Q.; Zhang, J.; Andersen, J. E. T.; Ulstrup, J. *J. Phys. Chem. B* **2001**, *105*, 4669.

(21) Armstrong, F. A.; Barlow, N. L.; Burn, P. L.; Hoke, K. R.; Jeuken, L. J. C.; Shenton, C.; Webster, G. R. *J. Chem. Soc., Chem. Commun.* **2004**, 316.

(22) Armstrong, F. A.; Hill, H. A. O.; Oliver, N. B.; Walton, N. J. *J. Am. Chem. Soc.* **1984**, *106*, 921.

(23) Bard, A. J.; Faulkner, L. R. *Electrochemical Methods*; J. Wiley & Sons: New York, 1980.

(24) Andolfi, L.; Bruce, D.; Cannistraro, S.; Canters, G. W.; Davis, J. J.; Hill, H. A. O.; Crozier, J.; Verbeet, M. P.; Wrathmell, C. L.; Astier, Y. *J. Electroanal. Chem.* **2004**, *565*, 21.

(25) Chi, Q.; Zhang, J.; Jensen, P. S.; Christensen, H. E. M.; Ulstrup, J. *Faraday Discuss. Chem. Soc.* **2005**.

(26) Du, H.; Strohsahl, C. M.; Camera, J.; Miller, B. L.; Krauss, T. D. *J. Am. Chem. Soc.* **2005**, *127*, 7932.

(27) Holmes, M. W.; Adams, D. M. *ChemPhysChem* **2004**, *5*, 1831.

(28) Yan, P.; Holman, M. W.; Robustelli, P.; Chowdhury, A.; Ishak, F. I.; Adams, D. M. *J. Phys. Chem. B* **2005**, *109*, 130.

(29) Bard, A. J.; Fan, F. R. F. *Acc. Chem. Res.* **1996**, *29*, 572.

(30) Mirkin, M. V.; Horrocks, B. R. *Anal. Chim. Acta* **2000**, *406*, 119.

(31) Laviron, E. *J. Electroanal. Chem.* **1979**, *100*, 263.